Open Access

Journal of Energy and Power Technology

LIDSEN Publishing Inc.

Original Research

Security Length Associated with the Risk of Ammonia Tank Leak Using CTOA Criterion and ALOHA Software

Kwami Eli Baba, Guy Pluvinage *, Julien Capelle

LEM3-ENIM, University of Lorraine, Nancy, France; E-Mails: kwami-eli.baba4@etu.univ-lorraine.fr; pluvinage.guy@orange.fr; julien.capelle@enim.univ-lorraine.fr

* **Correspondence:** Guy Pluvinage; E-Mail: pluvinage.guy@orange.fr

Academic Editor: Alfonso Chinnici

Journal of Energy and Power Technology
2024, volume 6, issue 4
doi:10.21926/jept.2404018

Received: August 06, 2024
Accepted: October 28, 2024
Published: October 31, 2024

Abstract

Ammonia is a toxic gas and can cause tragic consequences for humans. The damage level depends on concentration and duration of exposure. The security length associated with the risk of a tank leak at the acute exposure level of 30 ppm (AEGL-1) has been computed. Two tools have been combined: the CTOA criterion and the ALOHA software. The CTOA, a measure of fracture resistance against ductile crack propagation, is implemented in Abaqus software to compute the size of a breach in a tank submitted to internal pressure. This breach is assumed to be initiated by a gouge-dent defect provoked by a shock. The ALOHA software introduces the tank's characteristics, contents, and breach size. This allows us to determine and visualize the security length. The security length depends on geographic and climatic conditions, and for an incident localized in Metz (France), a value of 436 m was found. The effects of internal temperature, wind speed, and breach position are studied. A comparison for the same reference state with hydrogen is also made.

Keywords

Ammonia; CTOA; ALOHA; security length; internal temperature; wind speed

1. Introduction

Using ammonia as a hydrogen carrier is a promising approach in the energy field [1]. (NH_3) is a molecule that can be produced on a large scale from hydrogen and nitrogen, two abundant components in the atmosphere. Once created, it can be stored and transported relatively quickly, making it an attractive hydrogen carrier for energy. In the energy context, several ways for the use exists:

- Hydrogen storage: It can store large quantities of hydrogen at relatively high energy densities. It can be stored in liquid form at moderate temperatures and pressures, making it more practical than storing compressed or liquefied hydrogen gas [2].
- Hydrogen Transportation: It can be transported by pipeline, tanker truck, or ship, providing an alternative to liquid or gaseous hydrogen transportation infrastructure.
- Fuel [3] can be used directly in internal combustion engines or fuel cells. When burned, it produces only water and nitrogen as combustion products, making it cleaner than traditional fossil fuels.

It can be used for hydrogen production with much lower CO_2 production than steam methane reforming and coal gasification (7-29 kg and 14-60 kg CO_2 emissions per kg of hydrogen 1.6 to 1.8 and 2.5 to 3.8 tonnes of CO_2 per tonne produced).

Green hydrogen [4]: it can be produced from green hydrogen, that is, from renewable energy sources such as solar, wind, hydropower, and atmospheric nitrogen. This makes it a hydrogen vector compatible with an energy transition towards more sustainable and renewable energy sources.

(NH_3) has attracted much attention thanks to its high hydrogen content and ease of liquefaction under favorable temperature conditions: boiling point of -33°C under normal pressure conditions.

The risk of this gas causing combustion and explosion is much lower than that of other gaseous and liquid fuels, mainly hydrogen. Like most chemicals, ammonia is dangerous if inhaled and potentially fatal when exposed at a concentration between 2000 and 3000 ppm in the air within half an hour. The toxicity is associated with its high solubility and alkalinity, which results in solutions that make it an aggressive agent for mucous membranes and lungs [5]. It is easily detectable at a concentration above 5 ppm, emitting a pungent and suffocating odor. The smell becomes particularly penetrating beyond 50 ppm [6]. Standards for human exposure to this gas have been established and vary depending on legislation and duration of exposure.

Therefore, risk assessment and prevention are mandatory for the use and transportation. In 1990, an ammonia leakage in Cuba caused six deaths, and more than 400 people were intoxicated.

Hence, risk assessment is essential to the chemical sector. In 1990, an accidental ammonia leakage in the Cuban city of Matanzas caused six deaths, while more than 400 people were intoxicated [7]. In Brazil, the same type of incident occurred and caused the death of two workers and numerous intoxicated people [8]. In 2010, an ammonia leakage accident happened in the United States of America, and more than 120 people were intoxicated [9].

The failure initiation in a pressure vessel is generally followed by dynamic crack extension. Such disasters cause significant financial losses and mainly human risk due to the toxicity of the content, in the case of ammonia. It should be avoided as much as possible or limited to a short portion of the vessel. Therefore, an important question is if and when the fracture will stop. The propagation of brittle cracks can be successfully avoided using high-toughness steel; common ductile fracture remains the most critical failure mode. Dynamic ductile crack propagation occurs when the energy

of the driving force, caused by the internal pressure of the pipe, exceeds the resistance to crack propagation. In fracture mechanics, the resistance to crack propagation can be expressed by the experimental propagation resistance curve crack spacing R curve (CTOD) or crack opening angle (CTOA) [10, 11] as a function of the crack extension Δa.

The CTOA or crack opening angle is geometrically defined at the crack tip (Figure 1)

$$CTOA = \Psi = arctg\left(\frac{\delta}{d}\right) \quad (1)$$

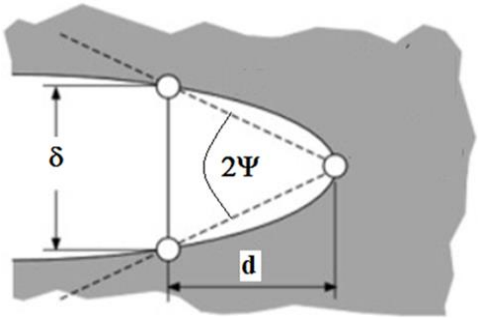

Figure 1 Definition of CTOA.

In terms of the limit state, the arresting pressure can be predicted by solving the equality between the vessel's toughness and crack opening stress, which depends on its dimensions, the internal pressure and the material. The arresting pressure can be predicted by solving the equality between the stress state at the crack tip and the local resistance to crack extension:

$$\langle \sigma_{ij}(p) \rangle = \langle \sigma_{ij,c}(p_{ar}) \rangle \quad (2)$$

where par is the stopping pressure. The following new condition can transform the arrest condition:

$$\mathrm{CTOA(p)} = \mathrm{CTOA_c(p_{ar})} \quad (3)$$

CTOA is the opening angle of the crack tip induced by the current pressure, and CTOAc is an expression of material toughness. A coupled gas-structure problem gives the conditions for crack propagation or arrest. Depressurization due to a crack opening will cause gas to flow out of the pipe. This induces depressurization waves propagating in opposite directions from the crack apices. The speed of crack propagation is controlled by the pressure distribution on the pipe [12]. If the decompression wave is faster than the crack propagation, the pressure at the crack tip will decrease, and the crack will stop.

This paper aims to calculate the necessary safety perimeter when a truck transporting gaseous ammonia is subject to a significant leak. For this, we use 2 essential elements: the concept of CTOA and security perimeter calculation software called ALOHA.

The procedure is as follows:

- Calculation of the conditions for initiating a rupture from a pre-existing defect consisting of a dent combined with scratching,
- Calculation of the fracture propagation conditions using the CTOA concept,
- Calculation of the conditions for crack arrest, calculation of the breach surface,
- Calculation of the conditions for the flow of gas escaping from the reservoir,

- Application of ALOHA software for calculating the security perimeter.

2. ALOHA Software

ALOHA (Areal Locations of Hazardous Atmospheres) is a standalone application software developed and supported by the National Oceanic and Atmospheric Administration (NOAA) in collaboration with the Environmental Protection Agency (EPA). Its main objective is to estimate the extent of spatial hazards linked to chemical spills [13]. It is applicable when wind speed is greater than 1 meter per second at a height of 10 meters, and it is unsuitable for very low wind speeds or calm conditions [14].

ALOHA uses two dispersion models: dispersion Gaussian and the dispersion of heavy gases. He chooses between the two based on chemical properties and the quantity of gas. A gas heavier than air is determined based on its molecular weight. Ammonia is a gas lighter than air but behaves like a heavy gas if released from a liquefied state [15]. The ammonia is in liquid form in the tank; therefore, the heavy gas model is the model of choice for all calculations performed. It is based on the DEGADIS model [16]. The movement of air above the blanket generates a dense column of gas. The cover is described as a cylindrical volume of gas extending laterally. To facilitate the calculations, the cylindrical cover is considered a square prism with the same volume and height. We assume the column comprises a homogeneous horizontal core with a width of 2b, presenting a vertical dispersion and edges of Gaussian distributions. As the column evolves from stratified shear flow stable towards passive turbulent diffusion, the width of the homogeneous core gradually decreases until it becomes zero.

The following equation, which expresses the pollutant's concentration, applies in both regions.

$$C(x,y,z) = c_g \exp\left[\left(-\frac{|y| - b(x)}{s_z}\right)^2 - \left(\frac{z}{s_z}\right)^{1+n'}\right] \; if \; |y| > b \qquad (4a)$$

$$C(x,y,z) = c_g \exp\left[-\left(\frac{z}{s_z}\right)^{1+n'}\right] \; if \; |y| \leq b \qquad (4b)$$

With

- c_g: the concentration at ground level in the central axis (ppm),
- S_y: the lateral dispersion parameter (m),
- S_z: the vertical dispersion parameter (m),
- b: the half-width of the homogeneous section of the core (m),
- constant n’ in the wind profile according to the power law.

3. Vessel and Material

Cargo tanks are widely used worldwide for ammonia transportation, usually for distances less than 150 km. This characteristic is a consequence of the relatively higher cost of this method compared with the other transportation modes in North America, ammonia is transported in MC331 cargo tanks as a pressurized liquid [17]. In Germany and other European countries, liquid and aqueous ammonia tank cars have a volume of 100 and 30 m^3, respectively [18]. The dimensions of the studied tank are given in Table 1.

Table 1 Dimensions of the studied tank.

Volume	Total length (m)	External diameter (m)	Wall thickness (m)
30 m^3	16.7	1.567	0.0158

The service pressure is 2 MPa. At this pressure and a temperature of -40°C, the ammonia density is 689.93 Kg/m^3; therefore, the ammonia weight is 20.7 tons. At the service pressure, the stress state is given in Table 2.

Table 2 Stress state of the tank.

Circumferential stress $\sigma_{\theta\theta}$	Longitudinal stress σ_{zz}	Von Mises stress σV_m
98.7 MPa	49.3 MPa	83.7 MPa

The vessel is assumed to exhibit a failure precursor as a gouge-dent defect made by shock. An example of an actual gouge-dent defect is given in Figure 2. The dimensions of the gouge-dent defect are given in Table 3 and Figure 3.

Table 3 Dimensions of the gouge-dent defect.

Dent depth	Dent length	Dent width	Gouge length	Gouge depth	Gouge width
d_d = 40 mm	l_d = 600 mm	W_g = 600 mm	2a = 310 mm	d_g = 7.9 mm	2c = 2 mm

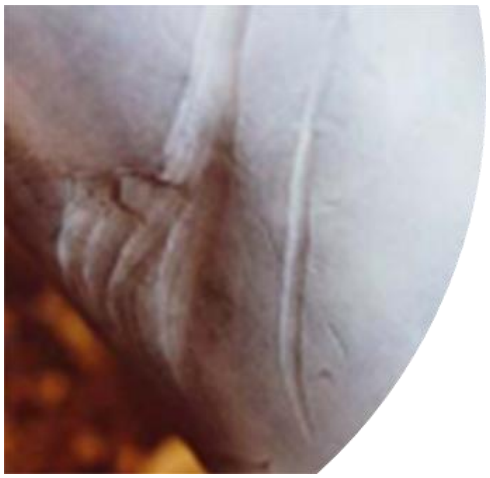

Figure 2 Example of a gouge-dent defect in a tank.

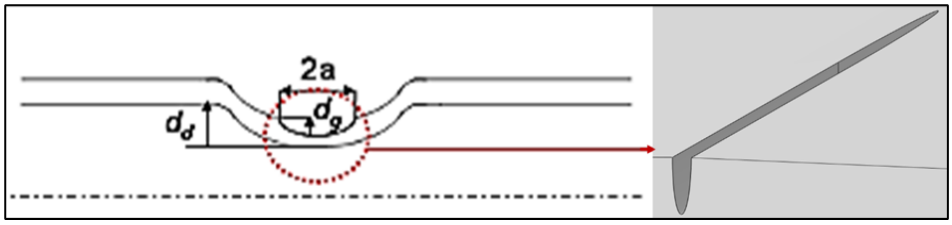

Figure 3 Geometry of the gouge-dent defect.

The gouge in the present study can be compared to a semi-elliptical notch l. It has a length of 2a = 310 mm, a width of 2c = 2 mm, and a depth d_g = 7.9 mm, corresponding to half the tank's thickness with a radius at the end of the notch ρ = 0.25 mm.

The vessel is made of A 285 carbon steel. This material has the following mechanical properties, Table 4. Material data are extracted from [19].

Table 4 Mechanical properties of A 285 carbon steel.

Yield stress σ_0 (MPa)	Ultimate strength σ_{ul} (MPa)	Young's modulus (GPa)
251	415	207

The stress-strain curve of steel A285 is described by the Randberg-Osgood law, Figure 4.

$$\varepsilon = \frac{\sigma}{E} + \alpha \frac{\sigma}{E}\left(\frac{\sigma}{\sigma_0}\right)^{N-1} \tag{5}$$

Where σ: true stress, ε: true strain, E: Young modulus, strain hardening coefficient α = 3.2, yield stress σ_0 = 251 MPa, strain hardening exponent $N = 5$.

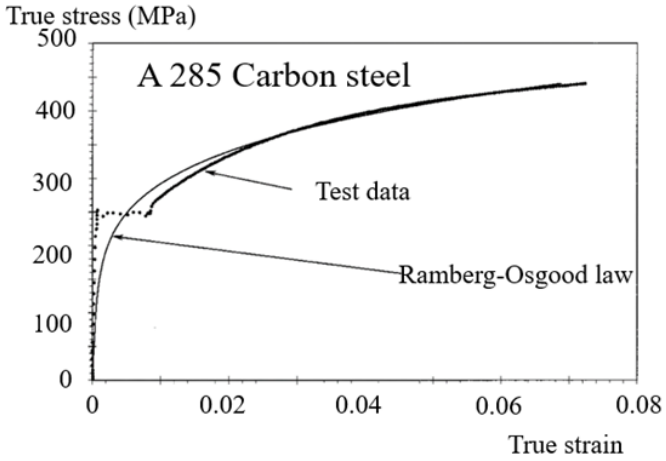

Figure 4 Stress-strain curve of A 285 carbon steel [19].

The critical CTOA values depend on specimen geometry and loading through constraint. Xian - Shui Zhu et al. [19] have proposed a relationship between the critical CTOA (CTOAc) value and constraint parameter A_2.

The stress distribution at the crack tip is described by the HRR solution for elastoplastic materials [20]:

$$\frac{\sigma_{ij}}{\sigma_0} = \left(\frac{J}{\alpha\sigma_0\sigma\varepsilon_0 I_N L}\right)^{1/N+1}\left[\left(\frac{r}{L}\right)^{s_1}\widetilde{\sigma_{ij}}^{(1)}(\theta) + A_2\left(\frac{r}{L}\right)^{s_2}\widetilde{\sigma_{ij}}^{(2)}(\theta) + A_2^2\left(\frac{r}{L}\right)^{s_3}\widetilde{\sigma_{ij}}^{(3)}(\theta)\right] \tag{6}$$

The J Integral governs the stress distribution. This fracture mechanics concept measures the strain energy release rate at the crack tip. This energy rate is the difference between the work done and the strain energy stored in the cracked body. The first is a volume integral, and the second is a

surface integral. For commodity, the difference is presented as a contour integral called J. At fracture, J reaches a critical value of J_c.

One of the parameters of the HRR solution A_2 is considered a measure of constraint [20].

The stress angular functions $\widetilde{\sigma_{ij}}^{(k)}(\theta)$ (k = 1, 2, 3) and the stress power exponent s_k (k = 1, 2, 3) depends on the strain hardening exponent N = 5. L is a characteristic length L = 1 mm, and σ_0 the yield stress ε_0 the associated elastic strain, ε_0 = 0.001213, σ_0 = 251 MPa. The J Integral value is calculated as J = 433 kJ/m2 as a notch J integral. It is an integration constant for N = 5, I_N = 5, 03769.

The A_2 parameter, which characterizes the constraint for the elastoplastic stress distribution as the T stress for the elastic one, has the value A_2 = -0.531.

For the A 285 carbon steel, the relationship between critical CTOA (Ψ_c) and constraint A_2 is linear [19]:

$$\Psi_c = -19.337A_2 + 6.215(degree) \quad (7)$$

Which gives a value of $\psi_c = 16.48°$. This value will be used in our FEM computing.

4. Evaluation of the Breach Size

The value of the gas flow passing through the hole caused by pipe failure is related to the size of the breach. To obtain the breach size, the Finite Element Method has been used to describe the phenomenon of crack propagation and arrest and to identify its dimensions i.e. length 2c and width 2a, assuming that its shape is elliptical.

A method based on the CTOA criterion to compute the size of a breach in a pipe submitted to internal pressure has been developed previously [11, 12, 21].

The breach development is simulated using Abaqus software. Crack propagation is allowed when CTOA reaches a critical value. On Abaqus, this is associated with the releasing nodes technique of each element to simulate the crack propagation. New digital conditions are necessary to implement this approach in a 3D model.

The implementation needs the following steps:

- The vessel with the geometry and the dimensions described previously is meshed. It exhibits a dent depth combined with a semi-elliptical gouge. This combined defect promotes failure at the service pressure of 2 MPa by a stress concentration. The local opening stress is higher than the failure strength. After fracture initiation, a crack is considered at the tip of the gouge.
- The boundary conditions corresponding to the symmetry concerning X and the symmetry condition of Z are only directly applied to a part of the corresponding surface. They are dedicated to the propagation of the crack. It will, therefore, be on this surface that the nodes must be released. Elements of 1 mm size are applied to this surface and the gouge area. With 7 elements in the thickness, the total number of elements is 614393.
- Sets of nodes are created on this surface. Each set is a set of 8 nodes in the thickness of the tank. Each has symmetry conditions associated with them concerning Z (Figure 5).

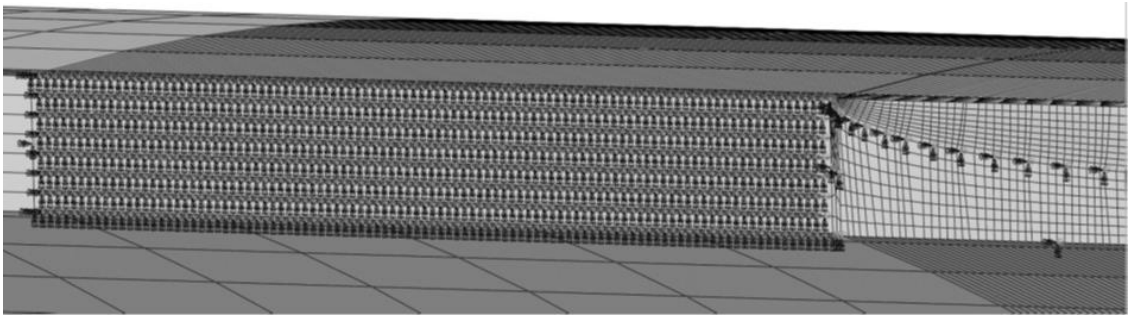

Figure 5 Meshing of the tank plate and the gouge.

- Step by step, the symmetry conditions are applied to the sets of nodes freed from any constraints.

All the steps mentioned above were iterative, and Python scripts were used to automate them. Finally, to evaluate the angle at the crack tip, another Python script allows for the reading of the database file (.odb) by retrieving the coordinates of the nodes of each set at each stage of the simulation. Following each release of nodes, a pressure drop is applied. After different simulations, the 0.5% pressure drop criterion is chosen because the evolution of the CTOA during propagation remains quasi-constant and drops rapidly near the arrest length.

At the end of propagation, the breach has the following dimensions a = 299.5 mm and c = 1.35 mm. It is assumed to be elliptic with a surface area $S \backsimeq 1270\ mm^2$.

5. The Security Length Given by ALOHA Software

To determine the security zone, ALOHA needs input data. They include the location of the site, atmospheric parameters, and the characteristics of the damaged reservoir. These data correspond to a “reference state” and are summarized in Table 5.

Table 5 “Reference state” parameters for Ammonia.

Parameters	Input
Location	Metz France
Elevation (meters above sea level)	220
Latitude	49°5’ North
Longitude	6°13’ East
*Wind speed (m/s)	5
wind direction	West
Wind measurement height (m)	10
* Cloud cover (1-10)	Partly covered (6)
* Air temperature (°C)	10.5
Thermal inversion (YES/NO)	NO
* Humidity (%)	76
Roughness	Urban/forest area
Tank volume (m^3)	30
Internal pressure (MPa)	2
* Internal temperature (°C)	-40

Fill rate (%)	100
* Position of the breach	On the side

(*) These parameters will be discussed later.

The impact zones have been determined using Aloha software for the 3 security levels for ammonia, which was given by another standard, the American Environmental Protection Agency, which also defined three levels of safety as shown in Table 6 [6].

Table 6 Indicative levels of acute exposure in ppm (AEGL-Acute Exposure Guideline Levels).

	10 mins	30 mins	1 hr	4 hrs	8 hrs
AEGL-1	30 ppm	30 ppm	30 ppm	30 ppm	30 ppm
AEGL-2	220 ppm	220 ppm	160 ppm	110 ppm	110 ppm
AEGL-3	2700 ppm	1600 ppm	1100 ppm	550 ppm	390 ppm

The lower level (AEGL-1) with 1-hour exposure time has been chosen for health prevention. In this case, the maximum length of the security zone is 436 m in the wind direction.

Visualization of the 3 security zones associated with the three AELG levels is presented in Figure 6a and Figure 6b.

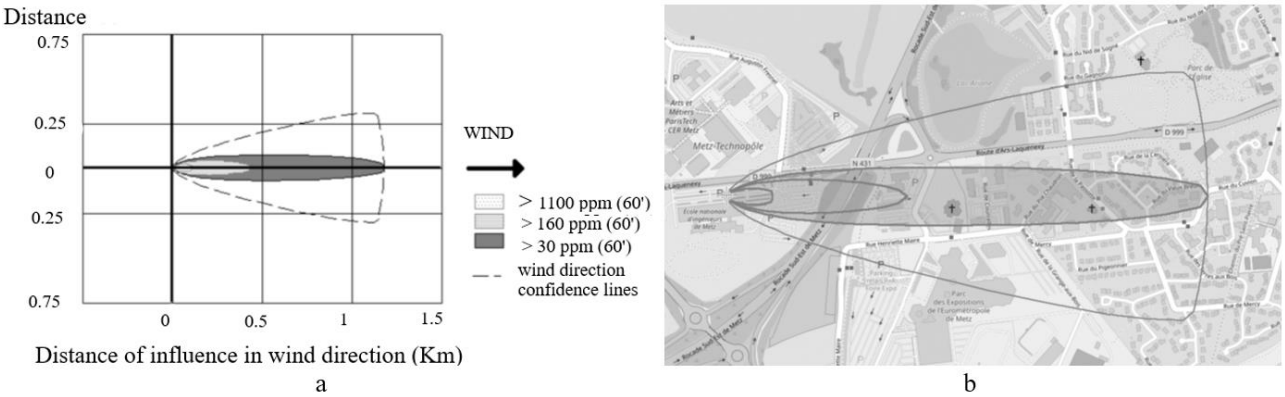

Figure 6 a: Ammonia: the 3 Impact zones for the reference state. b: Ammonia: Geographic visualization of the security zone (Metz France).

The security length is defined as the maximum length of the security zone. This length is in the wind direction. Conventionally, it is defined as the lower level AELG-1 and one hour of exposure, for health prevention considerations.

For the reference state defined in Table 5, this security length is 436 m.

6. Discussion

6.1 Influence of Atmospheric Parameters on Security Length

The following parameters mentioned in Table 5 are discussed: tank internal temperature, external temperature, cloud cover, and wind speed. Figure 7a, Figure 7b, Figure 7c, and Figure 7d

show how these parameters affect the security length. The security length of the reference state is 436 m.

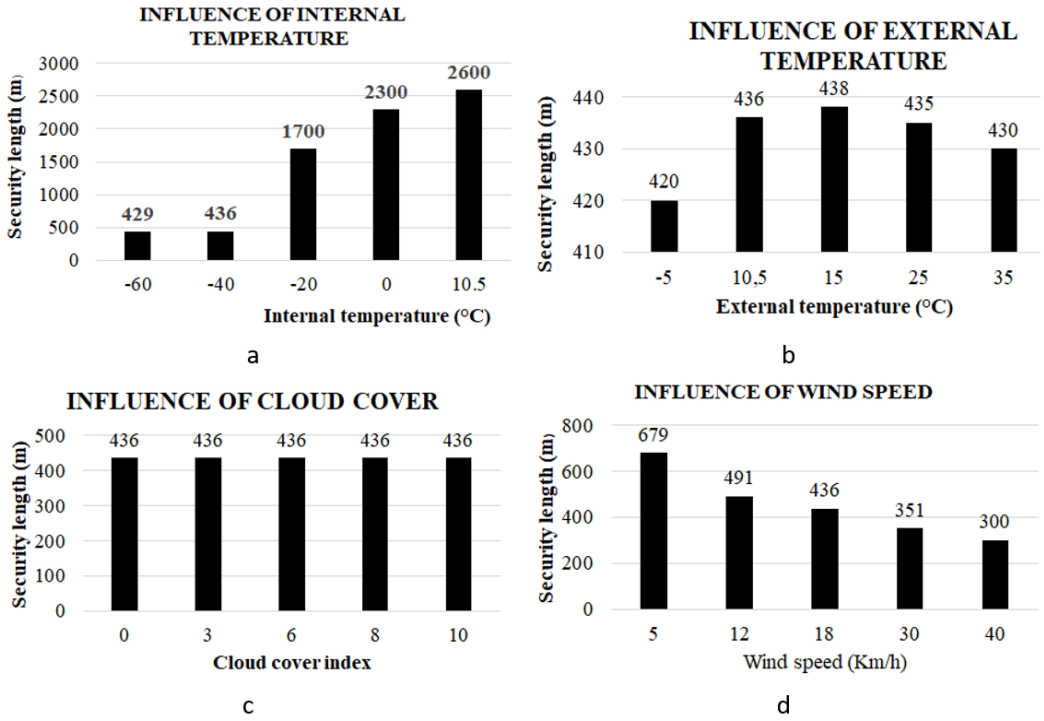

Figure 7 a: Influence of internal temperature on security length. b: Influence of external temperature on security length. c: Influence of cloud cover on security length. d: Influence of wind speed on security length.

In the tank, the internal temperature range is [-60°C–10.5°C], i.e., below and above the boiling temperature of ammonia (-33°C). The external temperature range is [-5°C–35°C], the cloud cover one [1–10], and the wind speed range [5–40 km/h].

One notes that the internal temperature strongly affects security length, which increases when the internal temperature increases. The external temperature has little effect and the cloud cover has no effect. The security length decreases when the wind speed increases due to ammonia dispersion. Two breach positions are considered: side and top, Table 7. A breach on the side gives a higher security length because there will be more leakage of liquid ammonia; on the top, much of the escaping ammonia is gaseous.

Table 7 Influence of breach position on security length.

Breach position	On side	top
Security length (m)	436	282
Δ (%)	0	-35.32

6.2 Comparison of Security Length When Using Pure Hydrogen or Ammonia for Hydrogen Transport

Hydrogen is emerging as one of the most efficient energy vectors. However, due to its explosive properties, Table 8, low density, storage, and hydrogen transport present significant challenges. Due

to its absence of carbon and the maturity of its production and distribution technologies, Ammonia represents an attractive alternative. However, the toxicity of ammonia raises safety concerns, requiring the application of strict measures in the event of leaks. A precautionary perimeter beyond which lethal risk is below a critical value becomes imperative for these two energy vectors. Therefore, comparing them from a strict point of view regarding security length is attractive.

Table 8 Ignition and flammability of hydrogen.

Auto-ignition temperature in air (°C)	Flammability limit in air (% vol)	Minimum ignition energy (mJ)	Burning rate in air ($m.s^{-1}$)
585	4-75	0.02	2.7

At atmospheric pressure, the hydrogen flammable range in the air is 4% to 75% by volume, which becomes explosive at 20% to 60%. An extremely low-energy ignition source can initiate combustion. A few seconds after the start of the hydrogen release, turbulent mixing between the hydrogen and the ambient air forms a cloud of flammable gas.

Due to the nature of hydrogen gas, the cloud of flammable gas produces an explosion and has a higher burn rate than other combustible gases. A gas cloud is formed after a pipeline failure occurs. Its flow increases rapidly by the impulse of the vented gas, and a quasi-steady gas jet is established. A blazing flare is produced if the released gas ignites immediately after the failure. A significant explosion occurs if the gas cloud is subjected to delayed ignition.

The prominent lethal risks can result from overpressure or the thermal effect of radiation caused by a sustained fire, which an explosion can precede. An explosion model of the gas cloud that characterizes the overpressure and a fire model that provides the intensity of the heat can be used to estimate the surface of the ground affected by a pipeline failure. The gas release rate of a failure is associated with the explosion's magnitude and the danger zone's corresponding size. The hydrogen release rate depends on the pipeline's service pressure, the pipeline, the length of the pipeline, and the adequate size of the hole. The diameter of the pipe, operating pressure, and pipeline length from the point of supply to failure determine the danger zone's parameters when the effective size of the hole is large, i.e., greater than the pipeline's diameter. The effect distance is integrated into the heat flux calculation and the determination of the overpressure value. Overall, this distance is defined as the distance between the source (gas cloud) and the target (the point considered for which people are present) [6]. This distance is determined using the equivalent TNT method [22].

In summary, although hydrogen and ammonia present risks associated with their handling and use, they differ in nature and intensity. Figure 8 presents a map of the plane flammability and toxicity of energy vectors: hydrogen, ammonia Natural gas, and fuel.

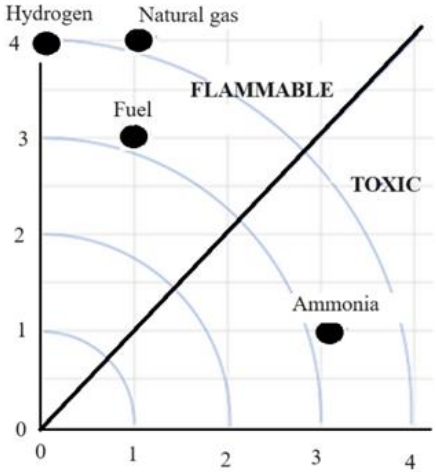

Figure 8 Maps in the plane flammability-toxicity of energy vectors.

In the following, the comparison of risks associated with the use of hydrogen or ammonia as an energy vector is based on the comparison of distance for the lethal effect.

In regulatory studies, three critical thresholds causing harmful effects on humans are retained for exposures of 1 to 60 minutes [23, 24]:

- Irreversible Effects (TIE) threshold, corresponding to the zone of significant dangers for human life, is 2 $kW.m^{-2}$ for thermal effects and 50 mbar for overpressure effects.
- The first Lethal Effects (TLE) threshold corresponds to the zone of severe dangers for human life, 5 $kW.m^{-2}$ for thermal effects and 140 mbar for overpressure effects.
- Significant Lethal Effects Threshold (SLE) corresponding to the zone of very serious dangers for human life, 10 $kW.m^{-2}$ for thermal effects, 200 mbar for overpressure effects.

The reference state defined earlier is taken over to compare the two energy vectors (Ammonia and Hydrogen). The ALOHA software modifies only the internal temperature (-250°C instead of -40°C) and the gas nature. The retained criterion for lethal effects is TIE. The security length is defined as the radius of the security zone. This length is independent of the wind direction for one hour of exposure. The security length for the hydrogen reference state is 610 m, as shown in Figure 9. This value is greater for hydrogen than for ammonia.

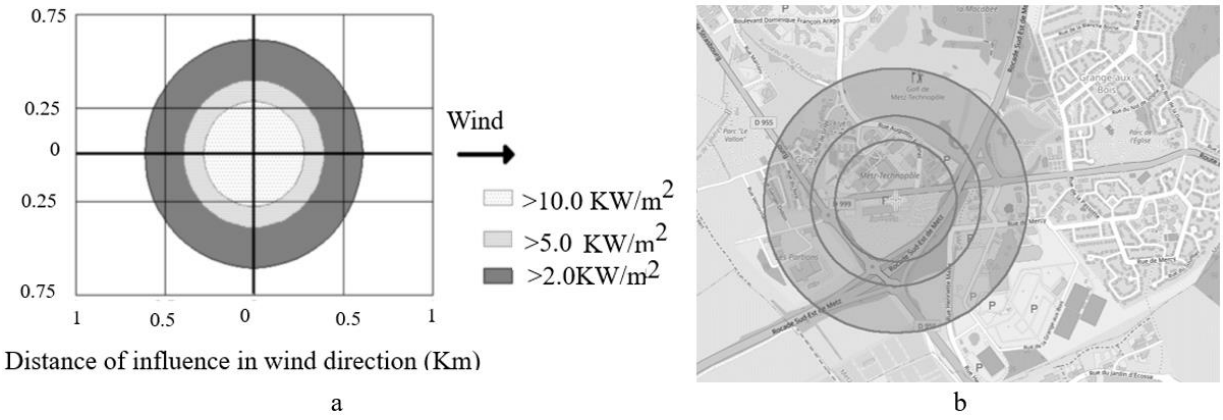

Figure 9 a: Hydrogen: the 3 Impact zones for the reference state. b: Hydrogen: geographic visualization of the security zone (Metz France).

The influence of tank internal temperature in the range [-258°C – -240°C] and wind speed in the range [5 km/h–40 km/h] have been studied. The security length decreases with moderation with the increase of temperature and the wind speed does not affect explosion and torch effect and therefore on security length, Table 9 and Table 10.

Table 9 Influence of internal temperature on security length (Hydrogen).

Internal temperature (°C)	-258	-250	-240
Security length (m)	636	610	505
Δ (%)	4.26	0	-17.21

Table 10 Influence of wind speed on security length.

Wind speed (km/h)	5	12	18	30	40
Security length (m)	610	610	610	610	610
Δ (%)	0	0	0	0	0

7. Conclusion

The security length associated with the risk of a leak in an ammonia tank is obtained using the CTOA criterion and the ALOHA software. This paper shows that the CTOA, a measure of fracture resistance against ductile crack propagation, is a tool for material selection and for computing the size of a breach for a tank filled with a gas or liquid under service pressure. It is associated with a particular FEM routine. ALOHA is a helpful software for determining and visualizing security lengths. It is based on the heavy gas plume model.

The security length is affected by internal temperature, wind speed, and breach position.

For the reference state described in this paper, the security length is 40% higher for hydrogen transport than ammonia.

Nomenclature

a	half of the gouge length
b	the half-width of the homogeneous section of the core
c	half of the gouge width
CG	concentration at ground level in the central axis
d	CTOA distance measurement
d_d	dent depth
d_g	gouge depth
l_d	dent width
n’	constant in the wind profile
s_k	stress power exponent
W_g	Dent width
y,z	coordinates
E	Young modulus
A%	Failure elongation

J	Integral for fracture toughness
L	characteristic length
N	strain hardening exponent
S_y	the lateral dispersion parameter
S_z	the vertical dispersion parameter
$\widetilde{\sigma_{ij}}^{(k)}(\theta)$	Stress angular functions
α	strain hardening coefficient
δ	Crack tip opening displacement
ε_0	elastic strain
σ_y	yield stress
σ_{ul}	ultimate strength$_0$
σ_0	flow stress
ψ	CTOA
Δ	relative error

Author Contributions

Conceptualization, G.P. and J.C.; methodology, J.C.; software, B.K.E.; validation, B.K.E., J.C. and G.P.; formal analysis, B.K.E.; investigation, B.K.E.; resources, J.C.; data curation, G.P.; writing—original draft preparation, B.K.; writing—review and editing, G.P.; visualization, J.C.; supervision, J.C.; project administration, J.C.; funding acquisition, J.C. All authors have read and agreed to the published version of the manuscript.

Competing Interests

The authors have declared that no competing interests exist.

References

1. Valera-Medina A, Banares-Alcantara R. Techno-economic challenges of green ammonia as an energy vector. New York, NY: Academic Press; 2020.
2. Elishav O, Mosevitzky Lis B, Valera-Medina A, Grader GS. Chapter 5 - Storage and distribution of ammonia. In: Techno-economic challenges of green ammonia as an energy vector. New York, NY: Academic Press; 2021. pp. 85-103.
3. Jeerh G, Zhang M, Tao S. Recent progress in ammonia fuel cells and their potential applications. J Mater Chem A. 2021; 9: 727-752.
4. Wang B, Li T, Gong F, Othman MH, Xiao R. Ammonia as a green energy carrier: Electrochemical synthesis and direct ammonia fuel cell-a comprehensive review. Fuel Process Technol. 2022; 235: 107380.
5. Bouet R. Ammoniac-essais de dispersion atmosphérique à grande échelle. INERIS rapport, ref lNERlS-DRA-RBo-1999-20410. 1999. Available from: http://www.ineris.fr/recherches/recherches.htm.
6. National Research Council, Committee on Acute Exposure Guideline Levels. Ammonia acute exposure guideline levels. Acute exposure guideline levels for selected airborne chemicals: Volume 6. Washington, D.C.: National Academies Press; 2008.

7. Orozco JL, Van Caneghem J, Hens L, González L, Lugo R, Díaz S, et al. Assessment of an ammonia incident in the industrial area of Matanzas. J Clean Prod. 2019; 222: 934-941.
8. Junior MM, e Santos MS, Vidal MC, de Carvalho PV. Overcoming the blame game to learn from major accidents: A systemic analysis of an anhydrous ammonia leakage accident. J Loss Prev Process Ind. 2012; 25: 33-39.
9. Tan W, Lv D, Guo X, Du H, Liu L, Wang Y. Accident consequence calculation of ammonia dispersion in factory area. J Loss Prev Process Ind. 2020; 67: 104271.
10. Mannucci G, Buzzichelli G, Salvini P, Eiber R, Carlson L. Ductile fracture arrest assessment in a gas transmission pipeline using CTOA. Proceedings of the 2000 3rd International Pipeline Conference, Volume 1: Codes, Standards and Regulations; Design and Constructions; Environmental; GIS/Database Development; Innovative Projects and Emerging Issues; 2000 October 1-5; Calgary, Alberta, Canada. New York, NY: American Society of Mechanical Engineers.
11. Ben Amara M, Pluvinage G, Capelle J, Azari Z. The CTOA as a parameter of resistance to crack extension in pipes under internal pressure. In: Fracture at all scales. Cham: Springer International Publishing; 2017. pp. 59-88.
12. Ben Amara M, Pluvinage G, Capelle J, Azari Z. Modelling crack propagation and arrest in gas pipes using CTOA criterion. In: Fracture at all scales. Cham: Springer International Publishing; 2016. pp. 171-194.
13. U.S. Environmental Protection Agency. ALOHA Software [Internet]. Washington D.C.: U.S. Environmental Protection Agency; 2024. Available from: https://www.epa.gov/cameo/aloha-software.
14. Jones R, Lehr W, Simecek-Beatty D, Reynolds M. ALOHA® (areal locations of hazardous atmospheres) 5.4. 4: Technical documentation [Internet]. Seattle, WA: National Oceanic and Atmospheric Administration; 2013. Available from: https://repository.library.noaa.gov/view/noaa/2669.
15. Anjana NS, Amarnath A, Nair MH. Toxic hazards of ammonia release and population vulnerability assessment using geographical information system. J Environ Manage. 2018; 210: 201-209.
16. Havens JA, Spicer TO. Development of an atmospheric dispersion model for heavier-than-air-gas mixtures, volume 1. Final Report. Fayetteville, AR: Arkansas Univ., Fayetteville Dept. of Chemical Engineering; 1985.
17. Colenbrander GW. A mathematical model for the transient behaviour of dense vapour clouds. 3rd International Symposium on Loss Prevention and Safety Promotion in the Process Industries; Basel, Switzerland. Bern, Switzerland: Swiss Society of Chemical Industries; 1980.
18. Russell AM, Becker AT, Chumbley LS, Enyart DA, Bowersox BL, Hanigan TW, et al. A survey of flaws near welds detected by side angle ultrasound examination of anhydrous ammonia nurse tanks. J Loss Prev Process Ind. 2016; 43: 263-272.
19. Zhu XK, Lam PS, Chao YJ. Constraint-dependent CTOA determination for stable ductile crack growth. Eng Fract Mech. 2022; 271: 108651.
20. Hutchinson J. Singular behaviour at the end of a tensile crack in a hardening material. J Mech Phys Solids. 1968; 16: 13-31.
21. Mijim JK, Pluvinage G, Capelle J, Azari Z, Benamara M. Probabilistic design factors for pipes used for hydrogen transport. Int J Hydrogen Energy. 2020; 45: 33860-33870.

22. Li S, Cheng C, Pu G, Chen B. QRA-grid: Quantitative risk analysis and grid-based pre-warning model for urban natural gas pipeline. ISPRS Int J Geoinf. 2019; 8: 122.
23. Ineris. Formalisation du savoir et des outils dans le domaine des risques majeurs (DRA-76) Ω-8 Feu torche. Rapport d'Etude N° DRA-14-133133-02917A. Paris, France: Ineris; 2014.
24. Sévêque JL. Étude de dangers des ICPE - Analyse des scenarios [Internet]. Saint-Denis, France: Techniques de l'Ingénieur; 2006. Available from: https://doi.org/10.51257/a-v1-g4211.